ELSEVIER

Ceramics International 28 (2002) 9–15

CERAMICS INTERNATIONAL

www.elsevier.com/locate/ceramint

Effect of silica fume addition on the properties of whiteware compositions

C.S. Prasad[a], K.N. Maiti[b], R. Venugopal[c,*]

[a]Central Glass and Ceramic Research Institute, Khurja Centre, Khurja 203131, India
[b]Central Glass & Ceramic Research Institute, Naroda Centre, 168 & 169, Naroda Industrial Estate, Ahmedabad 382330, India
[c]Indian School of Mines, Dhanbad 826004, India

Received 15 January 2001; received in revised form 27 February 2001; accepted 6 April 2001

Abstract

The effect of silica fume (SF) addition as a substitution of quartz on the thermo-mechanical properties and microstructure of traditional whiteware body compositions was studied. Noticeable improvement (10.0 + 0.5%) in the mechanical strength was observed on replacing quartz by 10% silica fume in whiteware body with the reduction of maturing temperature by 50 °C whereas addition of 25% silica fume reduced by 100 °C. The increase in strength has been attributed to the decrease in true porosity of the material as well as to the reduction of free quartz content in the composition. 34% Reduction of percentage thermal expansion at 600 °C was measured in the body mix containing 25% silica fume replacing quartz matured at 1150 °C, compared to the reference body matured at 1250 °C. The lower maturing temperature of the body would be helpful to reduce the fuel consumption and thus reduce production costs. © 2002 Elsevier Science Ltd and Techna S.r.l. All rights reserved.

Keywords: Silica fume; Properties; Whitewares

1. Introduction

Silica fume (SF), an anhydrous amorphous silica formed at high temperature and collected from the gas phase at voluminous, extremely finely divided powders. Fumed silica is made in one of the following ways [1]:

(a) Vaporising silicon dioxide in an arc or plasma jet and condensing it in a steam of dry inert gas.
(b) Oxidising the more volatile silicon monoxide in the vapour phase with air and condensing the SiO_2.
(c) Oxidising silicon compounds in the vapour state, such as Si H_4, $SiCl_4$ or H $SiCl_3$, with dry oxygen or in a hydrocarbon flame.

Silica fume is characterised by submicron particle size, flabby nature (thus behaving like a fume or smoke when dispersed in air), high surface area, spherical shape and glassy nature. Highly pure fumed silica in molten sphere form is commonly produced by oxidation of $SiCl_4$ vapour in an oxyhydrogen flame (also called "flame hydrolysis") [2].

$$2H_2 + O_2 — 2\ H_2O$$

$$SiCl_4 + 2\ H_2O — SiO_2 + 4\ HCl$$

$$SiCl_4 + 2H_2 + O_2 — 1800\ ^\circ C — SiO_2 + 4\ HCl$$

Molten spheres of silica thus produced (7–30 nm diameter) hit one another and form aggregates of ~0.03 μm size having extremely low bulk density (near by 0.03 g/cm^3). It controls the rheological properties of slip and serves as a reinforcing agent in adhesives and other resin systems. It is used in diverse industries due to its unique properties.

Quartz is used in almost all triaxial whiteware bodies as a major crystalline phase. Quartz grains embedded in the glassy matrix of a porcelain have a deleterious effect on the mechanical strength mainly because of α-β quartz transformation during cooling [3–5] resulting in the development of stress around quartz grains which initiate fracture [6]. Due to change in volume of free silica during reconstructive and displacive transformation, the

* Corresponding author. Tel.: +91-57-38-45081; fax: +91-57-38-42501.

PII: S0272-8842(01)00051-7

thermo-mechanical properties of whiteware bodies change considerably as reviewed in detail [7].

Notable improvement in the mechanical properties of whiteware bodies was observed by several investigators [8–17] on the addition of sericitic pyrophyllite, kyanite, bauxite, sillimanite sand, alumina in substitution of quartz. On the other hand, the silica-rich glass favours the recrystallization of mullite at low temperature and its dissolution at high temperature [18].

It was reported [19] that the dissolved quartz in the glassy phase and phase precipitation is dependent on the silica particle size. Several authors [20–23] found improvement in the mechanical properties through the reduction of the particle size of quartz and non-plastic materials. Silica fume [24–32] is mostly used in cements, coatings, binders, castables etc. as an admixture to improve their properties.

As per literature survey, authors found that no any investigator studied the effect of silica fume in whiteware composition so far. Therefore, keeping this in mind silica fume was progressively incorporated with the replacement of quartz and its effects on the properties of whiteware compositions were studied in detail.

2. Experimental procedure

The raw materials selected were Amrapali china clay (Supra grade), potash feldspar and calcined quartz. All the raw materials are available abundantly in India and are being used for the production of whiteware ceramics in the country. Silica fume (SF) incorporated in the whiteware bodies was collected from M/S Pooja Enterprises, Mumbai which has a surface area 14 m^2/g. Calcined quartz and potash feldspar were ground separately in a ball mill by the wet process as per the standard practice to the fineness of around 300 mesh. The slurry was sieved, passed through a magnetic channel and dried. Silica fume was used as received from M/S Pooja Enterprises, Mumbai. The particle size distribution of ground materials as well as china clay and silica fume was determined by the Andreasen pipette method. Chemical and mineralogical analyses of the raw materials were carried out according to the standard procedure. A standard whiteware body mix CSR-1 was selected as the starting composition and silica fume was gradually incorporated into the body by replacing calcined quartz (Table 1).

The test specimens were extruded in a vacuum extruder (Edward & Jones, England) in the form of cylindrical bars of 1.5 cm in diameter and 15 cm in length. These specimens were dried and then fired between 1100 and 1300 °C at a temperature interval of 50 °C in an electric furnace under a heating rate of 3.5 °C/min with 1 h soaking. Plastic and dry properties such as water of plasticity, dry linear shrinkage, dry strength and bulk density of dried test specimens were determined as per standard procedure.

Table 1
Body compositions with progressive replacement of quartz with silica fume in a standard whiteware composition (Mass %)

Raw materials	Body mix No.					
	CSR-1	SF-1	SF-2	SF-3	SF-4	SF-5
Amrapali china clay	50	50	50	50	50	50
Ground potash feldspar	25	25	25	25	25	25
Calcined quartz	25	20	15	10	5	0
Silica fume	0	5	10	15	20	25

Fired properties of test specimens such as fired linear shrinkage, fired strength, water absorption, apparent porosity and bulk density were determined by standard methods. Thermal expansion of matured specimens were determined using thermo-mechanical analyser (TMA), Shimadzu, Japan, DT-30 Model, under a heating rate of 10 °C/min.

The major crystalline phases were identified by XRD and the micro-structural features were studied by SEM on fractured etched surfaces in 10% HF for 5 min were studied for the existence of different phases. Specimens, cleaned by ultrasonic vibration were coated with a thin layer of gold-palladium by sputtering. The coated surfaces were used for the above study under a STEREOSCAN S250 scanning electron microscope.

3. Results and discussions

Chemical and rational analyses of the raw materials used in the investigation were carried out (Table 2). The result showed 35.13 and 17.84% alumina in Amrapali china clay and potash feldspar respectively whereas quartz and silica fume contained lower amounts of alumina 1.90 and 1.53% respectively. Potash feldspar contained 12.29% K_2O and 2.75% Na_2O whereas silica fume contained 0.34% Na_2O only. Wet sieve analyses as well as particle size distribution of all the raw materials are presented in Table 3. Particle size distribution of ground non-plastic materials and silica fume are almost identical.

Plastic and dry properties of body mixes are presented in Table 4. Water of plasticity and dry linear shrinkage of body mixes increased gradually and bulk density of body mixes was observed in the range of 1.72–1.54 g/cm^3.

Fired linear shrinkages of test specimens are shown in Fig. 1. The standard body marked CSR-1 showed the maximum linear shrinkage of 11.68% in the fired specimens at 1250 °C whereas SF-5 body mixed with 25% silica fume showed 14.63% linear shrinkage at 1150 °C. The results showed gradually increase in fired shrinkage on the additions of silica fume. Changes in percentage

Table 2
Chemical and rational analyses of raw materials (mass %)

Constituents	Amrapali china clay (supra Gr.)	Potash feldspar	Calcined quartz	Silica fume
SiO_2	46.24	65.65	96.80	96.05
Al_2O_3	35.46	17.84	1.90	1.53
Fe_2O_3	1.16	0.16	0.10	0.39
TiO_2	0.76	Trace	Trace	Trace
CaO	1.58	0.20	0.15	Trace
MgO	0.08	0.24	0.02	0.60
Na_2O	0.10	2.75	0.46	0.34
K_2O	0.42	12.29	0.14	Trace
L.O.I.	14.10	0.84	0.40	0.90
Rational analysis				
Kaolinite	88.63	–	1.43	–
Quartz	3.10	2.70	93.47	–
Feldspar	3.33	96.27	5.00	–
Calcite	2.84	0.30	–	–
Others	2.09	0.67	0.10	–

Table 3
Particle size distribution of raw materials used for body formulation (mass %)

Particle size (in micron)	Amrapali china clay	Potash feldspar	Calcined quartz	Silica fume
Sieve analysis				
+150	0.10	0.06	0.14	0.00
−150+106	0.30	0.55	0.32	0.00
−106+75	0.35	0.20	0.50	0.10
−75+53	2.15	0.70	0.45	0.20
−53	97.10	98.49	98.69	99.70
By sedimentation technique				
Greater than 25 μm	7.0	2.5	5.0	2.0
Between 25 and 15 μm	6.0	10.0	8.0	6.5
Between 15 and 10 μm	4.0	5.5	14.0	7.5
Between 10 and 5 μm	10.0	11.5	9.0	7.5
Between 5 and 3 μm	11.0	22.5	12.0	5.5
Between 3 and 2 μm	8.0	11.0	14.0	3.0
Between 2 and 1 μm	8.0	15.0	18.0	6.0
Below 1 μm	46.0	22.0	20.0	62.0
Below 10 μm	83.0	82.0	82.0	84.0
Below 15 μm	87.0	87.5	87.0	91.5

Table 4
Plastic and dry properties of body mixes

Properties	Body Mix No.					
	CSR-1	SF-1	SF-2	SF-3	SF-4	SF-5
Water of plasticity, %	21.4	22.0	24.0	24.2	24.6	25.2
Dry linear shrinkage, %	3.62	3.62	4.06	4.49	5.26	5.26
Dry M.O.R. (kg/cm^2)	10.06	10.66	10.86	10.86	10.86	10.86
Bulk density, g/cm^2 (dry test piece)	1.62	1.71	1.64	1.58	1.55	1.54

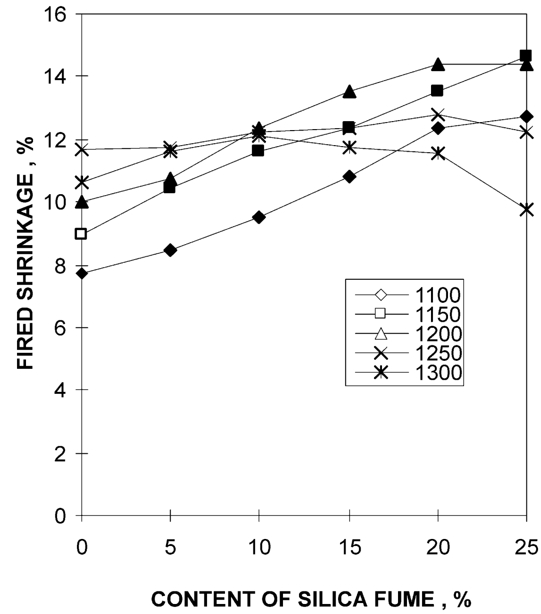

Fig. 1. Fired shrinkage of body mixes.

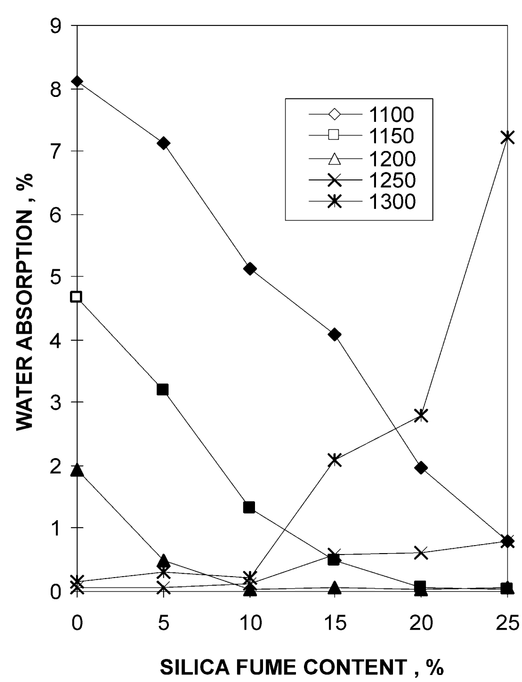

Fig. 2. Vitrification curves of different body mixes.

Table 5
Bulk density of different body mixes fired at different test temperatures

Temperature	Bulk density (g/cm^2)				
	1100	1150	1200	1250	1300
Mix No.					
CSR-1	2.03	2.18	2.28	2.38	2.36
SF-1	2.07	2.31	2.35	2.37	2.33
SF-2	2.19	2.36	2.41	2.41	2.34
SF-3	2.15	2.35	2.38	2.33	2.03
SF-4	2.27	2.37	2.40	2.36	2.06
SF-5	2.30	2.38	2.38	2.10	1.87

water absorption of fired test specimens are shown in Fig. 2. The curves clearly showed that the water absorption value of the body mix (CSR-1) fired at 1250 °C and the body mix (SF-5) fired at 1150 °C are below 0.05%. Hence the addition of silica fume in the body mix with the gradual replacement of calcined quartz decreased the maturing temperature.

The results of bulk density (Table 5) indicated that the standard body marked CSR-1 attained maximum bulk density 2.38 g/cm^3 at 1250 °C whereas body marked SF-5 attained maximum bulk density 2.38 g/cm^3 at 1150 °C. Maximum bulk density 2.41 g/cm^3 was observed in the sample containing 10 wt.% silica fume and fired at 1200 °C. Lower bulk density at 1300 °C indicated over firing of test specimens.

Thus, the addition of silica fume in the range of 10–25% was responsible for early maturing of test specimens by 50–100 °C as compared to that of standard body. Thus, whiteware bodies containing silica fume would attribute to the reduction of maturing temperature, thereby significantly saving fuel.

Fired strength of test specimens is shown in Fig. 3. All the bodies showed an increase in the fired strengths along with an increase in the test temperatures up to the point of respective maturing temperatures and then decreased due to over firing. The reference body containing 0 wt.%

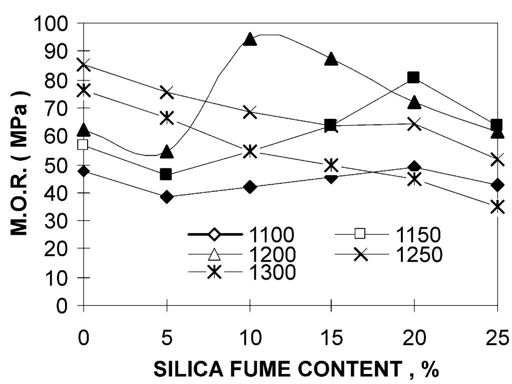

Fig. 3. Fired strength of body mixes fired at different test temperatures.

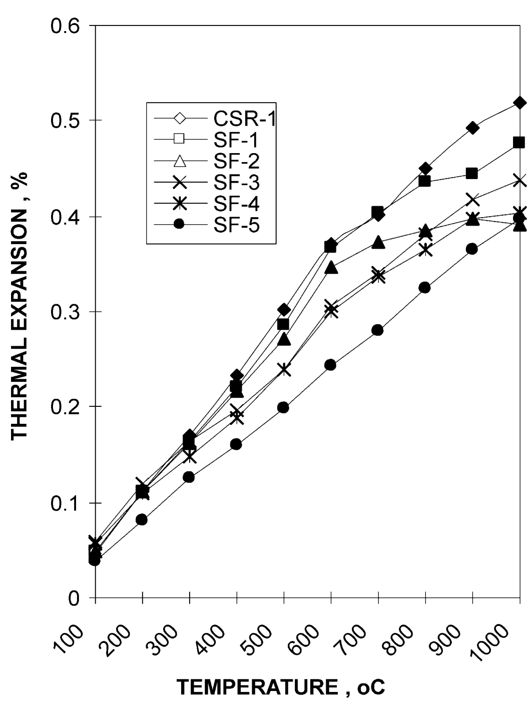

Fig. 4. Percent thermal expansion of matured body mixes.

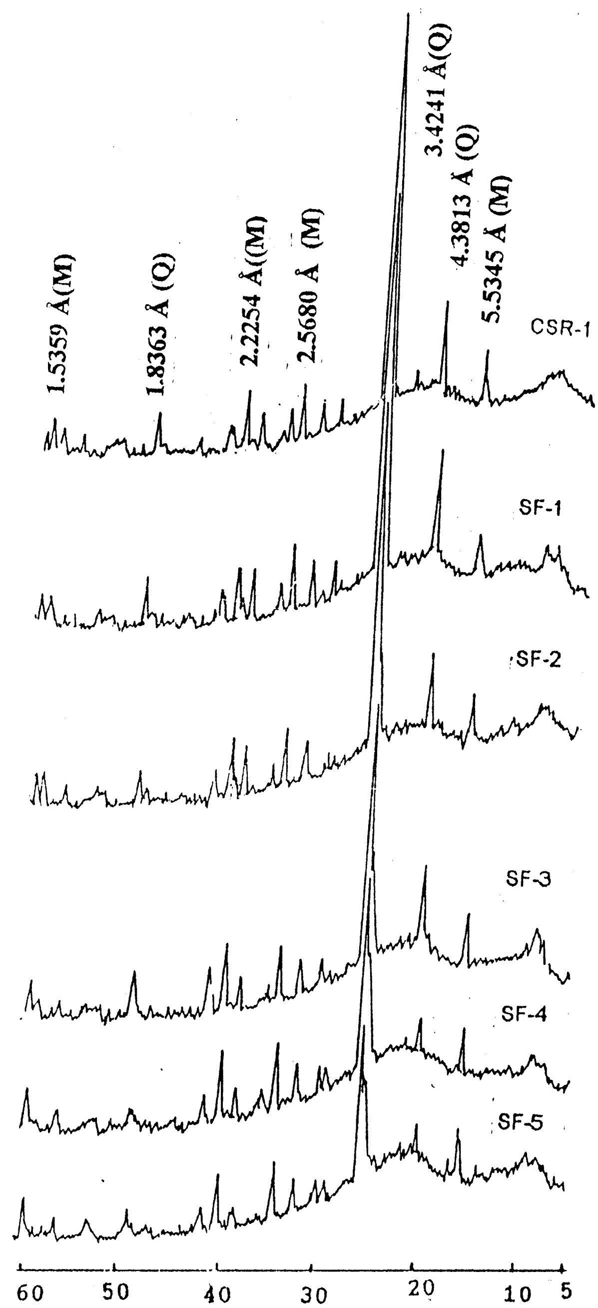

Fig. 5. XRD curves of fired body mixes (standard body mix CSR-1) and body mixes containing different proportions of silica fume, 5–25% in replacement of quartz (SF-1–SF-5).

silica fume showed the maximum fired strength of 85.6 MPa whereas bodies SF-2 and SF-5 containing 10 and 25 wt.% of silica fume showed the maximum fired strength 94.2 and 63.8 MPa in the samples fired at 1200 and 1150 °C, respectively. Decrease in the fired strength on addition of 25% silica fume might be due to the formation of a more glassy phase in the fired test specimens.

Thermal expansion of matured specimens (Fig. 4) decrease gradually with the addition of silica fume in the replacement of quartz. The removal of quartz from the mixes is primarily responsible for the decrease in the thermal expansion and for the disappearance of boundary stresses and hystersis at the quartz transformation temperature of 573 °C [21]. A reduction in the expansion of around 34.05% at 600 °C in the quartz free body (SF-5) in comparison to the reference body (CSR-1) was expected to enhance the thermal shock resistance of the specimens. A reduction in the thermal expansion (5.95%) in the body containing 10 wt.% silica fume was observed in comparison to the reference body (CSR-1). The bodies with little or no silica are also expected to eliminate dunting in whiteware.

Fig. 5 shows a powder X-ray diffraction pattern of matured samples. The curve marked CSR-1 shows that in the standard body composition, two major crystalline phases are present, namely mullite and quartz. The lines at 5.53, 2.57 and 2.22Å , are due to mullite. The lines at 4.38 and 3.42 , are due to quartz. On the addition of 25% silica fume in the complete replacement of quartz, the peak for quartz decreased significantly showing a reduction in the content of the free quartz in the fired specimen but the heights of the peaks for mullite remained almost identical to that of the reference body. These indicated that the addition of silica fume, decreased substantially the content of free quartz in the composition as also evident from a decrease in the percentage of thermal expansion, but the content of mullite did not increase significantly.

The SEM photographs of fracture etched surfaces of matured specimens of the standard body (CSR-1) and

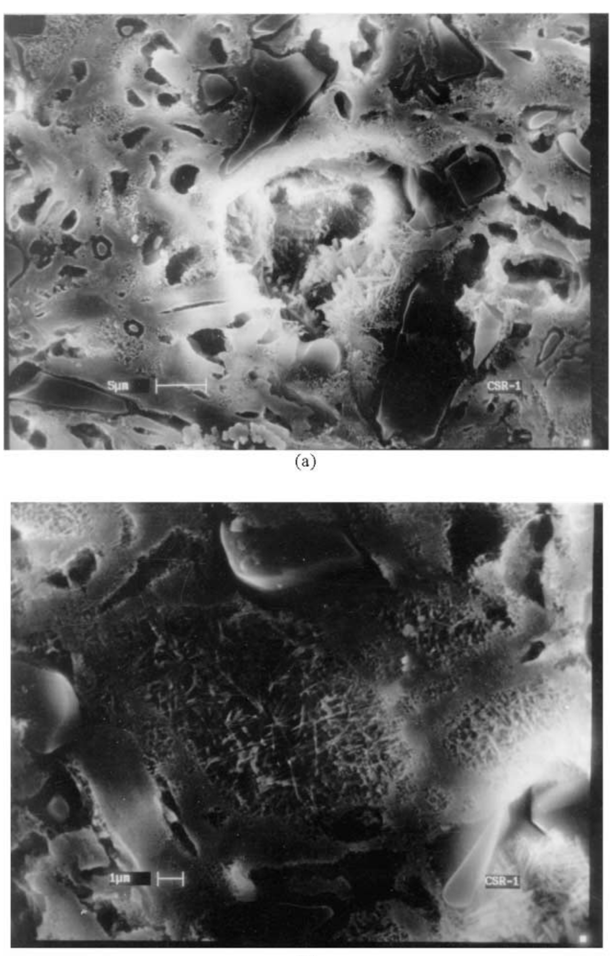

Fig. 6. (a and b). Occurrence of short and elongated mullite needles surrounded by other crystalline phases in the matrix, presented in different magnifications of standard body (CSR-1) fired at 1250 °C for 1 h.

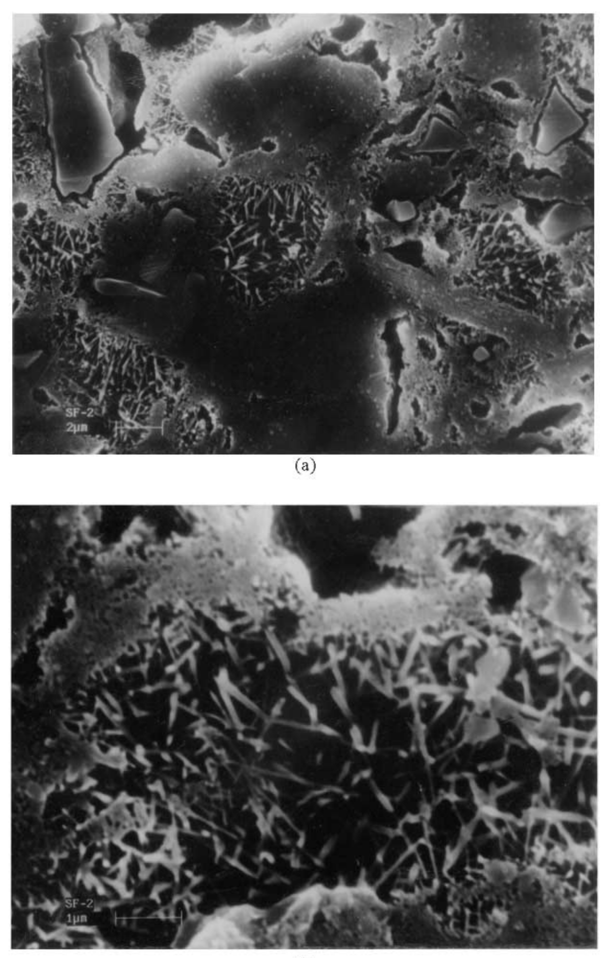

Fig. 7. (a and b). Micrographs showing recrystallised secondary mullite needles surrounded by other crystalline phases in the matrix of an SF-2 body containing 10% SF fired at 1200 °C for 1 h.

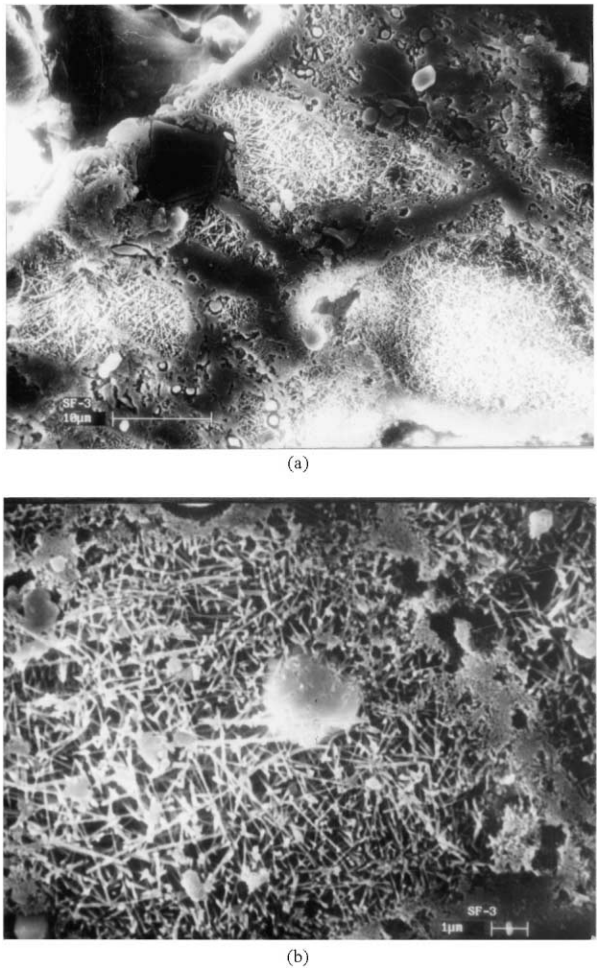

Fig. 8. (a and b). Occurrence of recrystallized secondary mullite needles, surrounded by other crystalline phases in the matrix of SF-3 body mix containing 15% SF fired at 1200 °C for 1 h.

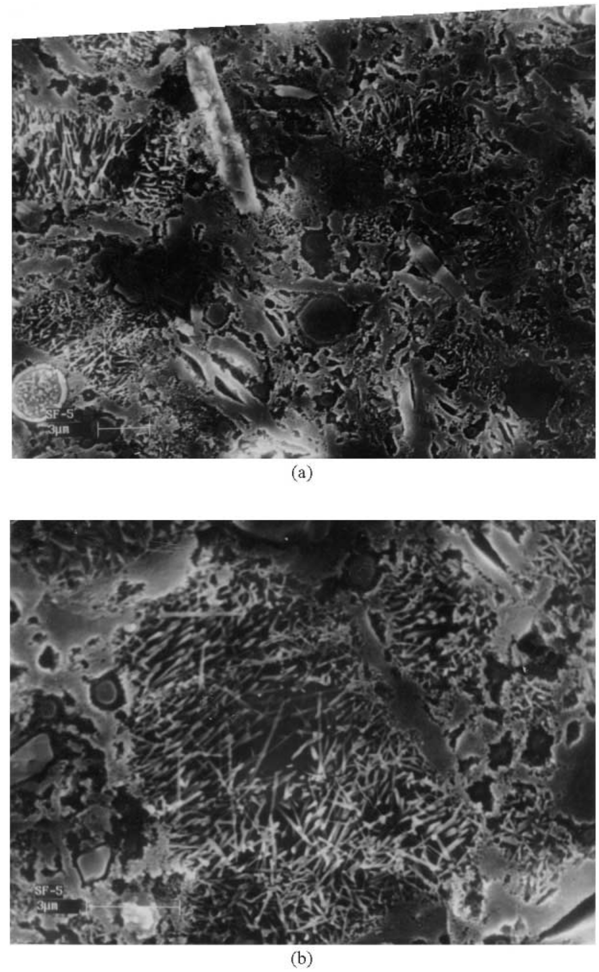

Fig. 9. (a and b). Crystalline phases with fine and long mullite needles in the matrix of SF-5 body mix containing 25% SF fired at 1150 °C for 1 h.

bodies containing 10, 15 and 25% silica fume are shown in Figs. 6 (a and b), 7 (a and b), 8 (a and b) and 9 (a and b), respectively. The micrograph (Fig. 6) shows unreacted quartz grains which are responsible for early failure of standard whiteware body upon mechanical and thermal stress [10,17]. The micrographs (Figs. 7 and 9) show a gradual reduction in unreacted free quartz in the matured test specimens which is due to the gradual addition of silica fume in the whiteware compositions.

Fig. 6 also shows the occurrence of short well interlocked mullite needles crystallised from the melt at the maturing temperature of 1250 °C along with pores. The specimens containing 10 and 15% silica fume (SF-2 and SF-3), matured at 1200 °C showed a large amount of fine recrystallised secondary mullite needles embedded in the glassy matrix which were extensively interlocked. These are also observed in the specimen containing 25% silica fume but fired at 1150 °C. The change in the size of mullite crystals due to the addition of silica fume might be due to dissolution and recrystallisation of mullite crystals in the glassy phase.

From the micrographs presented in Figs. 6–9, it is evident that in all the micrographs the major phases present were quartz and mullite apart from the glassy phase and the pores. However, the presence of pores and quartz relics appeared to be less in the micrographs especially with silica fume content and the minimum presence of pores and quartz relics were observed in the micrograph of SF-5.

4. Summary and conclusion

From the investigation, it seemed that incorporation of silica fume in place of quartz in whiteware bodies lowers the vitrification temperature. A reduction in the maturing temperature about 50–100 °C was noticed in the body mixes containing 5–25 wt.% of silica fume compare to that of the reference body. The increase in the fired strength about 10% with 10 wt.% silica fume and decrease in the thermal expansion (5.95%) are attributed to the sharp decrease in the content of quartz and also to the increase in the content of the glassy phase. However, the content of mullite appeared to be unaffected due to addition of silica fume in the compositions but with a change in the size of mullite crystals and its orientation as observed in the micrographs. The reduction in the vitrification temperature of the body mix containing 25 wt.% silica fume with a substantial decrease in percentage of thermal expansion (~34%) was observed which would contribute significantly to improvement to the economical production of whitewares.

Acknowledgements

The authors express their thanks to Dr. H.S. Maiti, Director, Central Glass and Ceramic Research Institute, Calcutta for his kind permission to publish this paper. Thanks are also due to Shri S. Chakrabarti, Scientist-in-Charge (Khurja Centre), Dr. (Mrs.) S. Sen and Dr. A. Chakraborty, Scientists for electron microscopy and X-ray diffraction data respectively.

References

[1] K.I. Ralph, The Chemistry of Silica, John Wiley & Sons, New York, 1979, pp. 21–29.
[2] M. Chatterjee, D. Ganguli, Powder preparation for advanced ceramics, in: S. Kumar (Ed.), Hand Book of Ceramics, Vol. I, Kumar & Associates, Calcutta, India, 1994, p. 119.
[3] H. Mortel, Influence of the batch composition on the reaction behaviour of fast fired (2 h) porcelain, Science of Ceramics 9 (1977) 84–91.
[4] I. Mattyasovzky, Mechanical strength of porcelain, J. Am. Ceram. Soc. 40 (9) (1957) 299–306.
[5] J.E. Schroeder, Inexpensive high strength electrical porcelain, Bull. Am. Ceram. Soc. 57 (1978) 526.
[6] S.I. Warshaw, R.J. Seider, in: R.M. Fulrath, J.A. Pask (Eds.), Ceramic Microstructures, John Wiley & Sons, New York, 1968, p. 559.
[7] W.D. Kingery, H.K. Bowen, D.R. Uhlman, Introduction to Ceramics, 2nd Ed., John Wiley & Sons, New York, 1976, pp. 506, 607–608.
[8] S.K. Khandelwal, R.L. Cook, Effect of alumina addition on crystalline constituents and fired properties of electrical porcelain, Am. Ceram. Soc. Bull. 49 (5) (1970) 522–526.
[9] L. Winnogradow, D. Kleinrock, M. Karp, Proc. 9th Conf. Silic. Ind. Budapest, 1968, p.407.
[10] K.N. Maiti, S. Kumar, Effect of substitution of quartz by beach sand sillimanite on the properties of conventional porcelain, Br. Ceram. Trans. J. 89 (1) (1990) 24–27.
[11] W.L. De-Keyser, Ber/Dtsch Keram. Ges. 49 (5) (1963) 304.
[12] C.S. Prasad, K.N. Maiti, R. Venugopal, Replacement of quartz and potash feldspar with sericitic pyrophyllite in whiteware composition, Interceram 40 (2) (1991) 94–98.
[13] C.S. Prasad, K.N. Maiti, R. Venugopal, Thermal behaviour of whiteware bodies containing sericitic pyrophyllite, Interceram 46 (3) (1997) 154–161.
[14] J.E. Hove, W.C. Rilley, Ceramics for Advance Technology, John Wiley & Sons, New York, 1991.
[15] A.A. Derevyagina, G.F. Derevyagina, B.I. Gaidash, Using kyanite sillimanite concentrate for making high tension porcelain, Glass Ceramic 37 (1980) 225–255.
[16] C.R. Austin, H.W. Schofield, N.I. Haldy, Alumina whiteware, J. Am. Ceram. Soc. 29 (12) (1946) 341–354.
[17] S.I. Warshaw, R. Seider, Comparison of strength of triaxial porcelain containing alumina and silica, J. Am. Ceram. Soc. 50 (7) (1967) 337–343.
[18] K.H. Schuller, Reaction between mullite and glassy phase in porcelain, Trans. J. Br. Ceram. Soc. 63 (1964) 103.
[19] M.F. Tomizaki, T. Sugiyama, Study of high silica porcelain bodies, Interceram 44 (4) (1995) 223–228.
[20] T. Sugiyama, T. Horiuchi, M. Tomizaki, H. Takashima, Study on high silica porcelain bodies, Interceram 44 (3) (1995) 139–145.
[21] A. Dinsdale, W.T. Wilkinson, Properties of whiteware bodies in relation to size of constituent particles, Trans. Br. Ceram. Soc. 65 (1966) 391.
[22] O. Krause, U. Klempin, Relationship between particle size of quartz and properties of hard porcelain—III, Aprechaal 75 (1942) (23–24) 229–231, (25–26) 251–255, (27–28) 273–276, (47–48) 400.
[23] K.N. Maiti, C.S. Prasad, Effect of particle size on the vitrification temperature and fired properties of conventional white stoneware, Trans. Indian Ceram. Soc. 48 (6) (1989) 119–127.
[24] S. Monosi, R. Troli, L. Coppola, M. Collepardi, Water reducers for the high alumina cement silica fume system, Mater. Struct. 29 (194) (1996) 639–644.
[25] M.P. Dallaire, N.S. Berke, Grace W.R & Co., Admixture for inhibiting drying shrinkage of cement, UK Patent, Apple. GB2305428A, W.R Grace & Co., 9 April 1997.
[26] E. Stav, E.A. Burkard, R.S. Finkelstein, Cementitious gypsum—containing composition and materials made their form, US Patent 5685903, Nationals Gypsum Co. 11 November 1997.
[27] M.S. Berke, M.P. Dallaire, Cement admixture, US Patent 5571319, W.R. Grace & Co., 5 November 1996.
[28] T. Yonezawa, K. Yanagibushi, Y. Tkeo, T. Okuno, E. Asakura et al., Hydraulic substance with water stable particle coating, US Patent 5584927, Takenaka Corp., Misubishi Materials Corp., Keihin Ryoko Concrete Industry Corp., Takemoto Oil and Fat Corp., 17 December 1996.
[29] J. Harald, Hydraulic binder based on condensed silica fume and slaked lime, Cement & Concrete Research, Trondheim, Norvey, Int. Congr. Chem. Cem., 9, 1992, Vol. III, pp. 284–290.
[30] Z.Z. Xu, P. Gu, P. Xie, J. Beaudoin, Application of ac impedance techniques in studies of porous cementitious materials; III ACIS (ac impedance spectroscopy) behaviour of very low porosity cementitious systems, J. Cem. Conc. Res. 23 (5) (1993) 1007–1015.
[31] Z. Bayasi, J. Zhou, Properties of silica fume concrete and mortar, ACI Mater. J. 90 (4) (1993) 349–356.
[32] J. Modej, J. Madejova, D. Jakubekova, IR spectroscopic study of hydration of condensed silica fume modified cement pastes, Ceram. Silik 34 (2) (1990) 131–141.